Impact of grain size on the convection of terrestrial planets

A. Rozel[1],

Abstract. This article presents a set of simulations of mantle convection, using a new model of grain size-dependent rheology. In the present paper, it is shown that this rheology behaves in many ways as a visco-plastic rheology. I use a model of grain size evolution which has been calibrated on experimental data in a previous paper. In this physical model, the grain size is directly related to the stress state, following a temperature-dependent piezometric law. The rheology used here allows both diffusion and dislocation creep, depending on the grain size. At low stress, the grain size is high and forces the rheology to be dislocation dominated. For sufficiently high stresses, the equilibrium regime reached by the grains is located in the diffusion creep. In this case, the viscosity is linked to a stress-dependent grain size, which actually makes the rheology more non-Newtonian than it is in dislocation creep. This experimentally calibrated model allowed me to perform a set of numerical experiments of convection in which the rheology may be diffusion or dislocation creep dominated, depending on the state of the stress tensor. Then, The stress exponent varies from 3 to 5 because of grain size, which has a large impact on the temperature dependence of the viscosity. The present paper shows the impact of this new model on the convection regimes of terrestrial planets. In particular, for a wide range of parameters, I observe the episodic regime which is thought to govern the dynamics of Venus. This process of episodic resurfacing was obtained in previous simulations using visco-plastic rheologies is a tight range of parameters. I obtain it here without using an ad hoc plasticity law, only using a viscous rheology based on laboratory measurements. In these simulations, I show that the cooling rate of the terrestrial planets may be largely modified by the consideration of a grain size-dependent rheology.

1. Introduction

Although the plate tectonic regime has been studied for decades, the rheologies that generate it self-consistently have still to be determined. Laboratory experiments of rock deformation show a strong effect of the temperature on the viscosity (see *Hirth and Kohlstedt* [2003]). But several studies have also shown that the consideration of a very temperature-dependent viscosity (in adequation with the experimental data) generates a stagnant lid on top of convection cells [*Christensen*, 1989; *Ogawa et al.*, 1991; *Solomatov*, 1995]. This might represent the convective state of Mars or Mercury but is very far from the plate tectonic regime of the Earth. Thus, it appeared that additional parameters are required to break the thick lithosphere generated by the huge temperature dependence of the viscosity.

Several effects have been proposed to localize the deformation at plate boundaries: plastic yielding [e.g., *Moresi and Solomatov*, 1998; *Trompert and Hansen*, 1998; *Tackley*, 2000], partial melting [*Bercovici and Ricard*, 2003; *McKenzie*, 1984], damage [*Bercovici et al.*, 2000; *Bercovici and Karato*, 2003], non-Newtonian rheologies [*Weinstein and Olson*, 1992], shear heating [*Burg and Schmalholz*, 2008], hydration of the rocks [*Lenardic and Kaula*, 1994; *Hilairet et al.*, 2007], etc. The singular state of the lithosphere of the Earth is probably due to a set of these potentially coupled parameters but the effect of each has still not always been systematically determined.

[1]LET Laboratory of Experimental Tectonics, Dipartimento Scienze Geologiche, Università Roma TRE, L.S.L. Murialdo 1; 00146 Roma, Italy. (antoinerozel@gmail.com)

Plastic yielding, instantaneous rheologies and shear heating seem insufficient to fully describe the behavior of the lithosphere of the Earth particularly because they do not provide an appropriate memory for the rheology [*Bercovici and Karato*, 2003]. Grain size dependent rheologies is used in several studies of the localization of deformation in shear zones [*Kameyama et al.*, 1997; *Braun et al.*, 1999; *Montési and Hirth*, 2003] or mantle convection simulations [*Hall and Parmentier*, 2003; *Barr and McKinnon*, 2007; *Solomatov and Reese*, 2008] but these formalisms are based on phenomenological considerations and lacks important physical properties such as energy conservation and the positivity of entropy evolution. Composite rheologies including dislocation creep, diffusion creep (and Peierls plasticity) have also been considered [*Kameyama et al.*, 1999; *Duretz et al.*, 2010] but the grain size is most often fixed to a constant value. Also, the value of the rheological stress exponent n (in the formalism $\underline{\dot{\epsilon}} \propto \tau^{n-1}\underline{\tau}$) is of primary importance in lithosphere scale simulations [*Bercovici*, 1993; *Montési and Zuber*, 2002].

Ricard and Bercovici [2009] proposed a new physical approach of the evolution of grain aggregates. This new theory allows to compute the dynamics of a grain size distribution in a very general way, consistent with the thermodynamic requirements. *Rozel et al.* [2010] used this general approach and calibrated it with the well-documented case of the olivine rheology (see also *Austin and Evans* [2007]). In the present paper, I use this rheology to investigate its effect on mantle convection. Note that the rheology is still not time-dependent in this new model because the grain size is obtained instantaneously from the stress state. [*Foley et al.*, 2012] have presented a set of simulations in which the viscosity depends on grain size using the formalism of *Ricard and Bercovici* [2009]. However, these simulations do not allow the rheology to switch from diffusion to dislocation creep following the stress magnitude, which is a central point of the present paper and modifies completely the dynamics of the whole mantle.

2. Setup

2.1. Framework of the convection experiments

I consider a fluid heated from below submitted to a temperature increase ΔT. The surface temperature is fixed to T_s and the bottom temperature to $T_b = T_s + \Delta T$. Except for the viscosity given by equation (17), all the other parameters are uniform. Top, bottom and side wall free slip boundary conditions are imposed and the aspect ratio of the domain is fixed to 1.

The Stokes equation is solved using the Boussinesq approximation, considering an infinite Prandtl number and the convecting material is considered incompressible. The Stokes, continuity, heat and grain size equations are given by:

$$\boldsymbol{\nabla} \cdot \underline{\boldsymbol{\sigma}} - \boldsymbol{\nabla} P = Ra_b T \boldsymbol{z} \quad (1)$$

$$\boldsymbol{\nabla} \cdot \boldsymbol{v} = 0 \quad (2)$$

$$\frac{\partial T}{\partial t} = \nabla^2 T - \boldsymbol{v} \cdot \boldsymbol{\nabla} T \quad (3)$$

$$\mathcal{R}_* = \zeta {\tau_*}^{-\frac{n+1}{p+1}} \quad (4)$$

where $\boldsymbol{v}$ is the velocity of the fluid, $\underline{\boldsymbol{\sigma}}$ is the stress tensor, P the pressure, Ra_b the bottom Rayleigh number (defined below, in equation 5), T the temperature, z the dimensionless depth and t the time. $\mathcal{R}_*$ is the dimensionless grain size, $\zeta = \chi/(\mathcal{R}_0 {\tau_r}^{-\frac{n+1}{p+1}})$, $\mathcal{R}_0$ is the reference grain size used to remove the dimension (1 micron), τ_r is the reference deviatoric stress (1 MPa) used to obtain the dimensionless second invariant of the deviatoric stress tensor τ_*. χ is a temperature-dependent variable defined in section 2.2, equation 10. n is the non-linear stress exponent and p an experimental dimensionless constant involved in the time-dependency of grain growth (see equation 7).

The structure of the convection code is fully described in *Trompert and Hansen* [1996] but I briefly summarize its main characteristics here. The equations 1, 2 and 3 are solved together using the finite volume formalism on a staggered grid defined in *Harlow and Welch* [1965]. The grid is uniform in the horizontal direction but very refined vertically in the top and bottom boundary layers. The vertical position of the mesh nodes are defined using a Chebichev polynomial. A grid of 64 times 64 nodes has been found to provide a satisfactory resolution. A multigrid solver is used to obtain velocity, pressure and temperature fields. The temperature equation is solved using the fully implicit Crank-Nicolson method. Smoothing iterations are performed with the SIMPLER method [*Patankar*, 1980]. Jacobi iterations are used to solve the temperature field and Gauss-Seidel iterations has been chosen to obtain the velocity field. W-cycles are performed to improve the convergence. As shown by equation 4 and explained in section 2.2, the grain size is obtained directly from the stress state and does not require any particular numerical treatment.

The bottom Rayleigh number is defined by:

$$Ra_b = \frac{\alpha \rho g \Delta T h^3}{\kappa \eta_b}, \quad (5)$$

where α is the thermal expansivity, ρ the density, g the gravity, h the depth of the computational domain, κ the thermal diffusivity and η_b is a bottom viscosity using the rheological parameters of the dislocation regime.

Because the rheology is non-Newtonian in the dislocation regime, the effective viscosity at the bottom of the convection domain cannot be known before running the simulation. Thus, following *Solomatov* [1995], I use

$$\eta_b = \frac{1}{2} \left(A_{10} \exp\left(-\frac{E_1}{R T_b} \right) \right)^{-\frac{1}{n}} {\dot{\epsilon}_0}^{\frac{1-n}{n}}, \quad (6)$$

where $\dot{\epsilon}_0 = \kappa / h^2$, A_{10} is a constant, E_1 is an activation energy (which quantifies the temperature dependence of the rheology), R is the Boltzmann constant and n is the stress exponent (in dislocation creep). This viscosity is defined with the bottom temperature T_b but with an a priori strain rate $\dot{\epsilon}_0$. The effective internal Rayleigh number obtained in my simulations is larger than Ra_b (the effective strain rate is much smaller than ϵ_0). The effective Rayleigh number, computed from the average internal viscosity, computed a posteriori, is about $10^6 - 10^7$. This formulation of the Rayleigh number based on the dislocation creep viscosity is very classical [*Solomatov*, 1995], I chose to use it as a starting point of my study.

Any attempt to run a convection experiment with Earth-like parameters would most probably fail. The viscosity variations occurring for a Arrhenius law between 300 K and 3000 K are incredibly huge (10^{59} for and an activation energy of 375 kJ mol^{-1}), and other phenomenon (e.g., brittle failure, Peierls mechanisms, damage...) would anyway limit the effective strength of the shallow layers. I did not consider these processes. In my simulations, I therefore restrict the temperature variations between $T_s = 1000$ K and $T_b = 2000$ K. Even in this case, the value of the activation energy is limited to 420 kJ mol^{-1} (see figure 2). The maximal viscosity contrast reached are already of the order of 10^{15}.

2.2. Grain size-dependent rheology

2.2.1. Approximation of the grain size kinetics

In *Rozel et al.* [2010], we derive the general evolution equation for the mean grain size $\mathcal{R}$, (equation (40) of *Rozel et al.* [2010])

$$\frac{d\mathcal{R}}{dt} = \frac{G}{p \mathcal{R}^{p-1}} - f \frac{\mathcal{R}^2}{3\gamma} \frac{\lambda_3}{\lambda_2} \underline{\boldsymbol{\tau}} : \underline{\dot{\boldsymbol{\epsilon}}}_{dis}, \quad (7)$$

where t is the time. The first term on the right is the usual coarsening term where $p \sim 2$ is an experimental dimensionless constant, and $G = k_0 \exp(-E_g/RT)$ is a kinetic term (see Table 1), k_0 is an experimental constant, E_g is the activation energy of the grain growth kinetics, T is the temperature in Kelvin. f is the partitioning parameter defined in equation 8, γ is the surface tension of the grain boundaries. λ_2 and λ_3 are dimensionless constants derived analytically in *Rozel et al.* [2010] (see table 1). $\underline{\boldsymbol{\tau}}$ is the deviatoric stress tensor and $\underline{\dot{\boldsymbol{\epsilon}}}_{dis}$ is the strain-rate tensor due to dislocation creep rheology only.

The first term of the right hand side of equation 7 represents the usual normal growth [e.g. *Hillert*, 1965; *Karato*, 1989]. The second term represents the effect of dynamic grain reduction through recrystallization. This term is controlled by the energy dissipated by dislocation creep, $\underline{\boldsymbol{\tau}} : \underline{\dot{\boldsymbol{\epsilon}}}_{dis}$ (contraction of the stress tensor $\underline{\boldsymbol{\tau}}$ and the strain rate tensor in dislocation creep $\underline{\dot{\boldsymbol{\epsilon}}}_{dis}$) and depends on γ, the surface tension of the olivine grains. We obtained the partitioning parameter f from various experiments and its temperature dependence may be reasonably approximated by:

$$f = \exp\left(-\alpha_f \left(\frac{T}{1000} \right)^{\beta} \right). \quad (8)$$

All the constants, α_f, β and λ_i are dimensionless. Their values are discussed from theory or observations (see *Rozel et al.* [2010]) and reported in Table 1.

The calibration of the grain size dynamics with experimental data shows that the kinetics of equilibration is rapid with respect to a typical convection time scale except on

the coldest, shallowest part of the lithosphere where deformation occurs anyway by different processes [*Rozel et al.*, 2010]. This result is based on the grain growth kinetics obtained by *Karato* [1989]. Thus, I have chosen to investigate the equation (7) in steady state, i.e., considering $d\mathcal{R}/dt = 0$. In this situation, the equilibrium grain size becomes:

$$\mathcal{R} = \chi(T)\tau^{-\frac{n+1}{p+1}}, \tag{9}$$

with

$$\chi(T) = \left(\frac{3\gamma G\lambda_2}{pfA_1\lambda_3}\right)^{\frac{1}{p+1}}, \tag{10}$$

where τ is the second invariant of the deviatoric stress tensor and A_1 is the dislocation creep rheological function given by $A_1 = A_{10}\exp(-E_1/RT)$.

Equation (9) is what is called a "pieozemeter" used by geologists to infer paleo-stresses from mineral grain sizes [e.g., *Van der Wal et al.*, 1993; *Post and Tullis*, 1999; *Shimizu*, 2008]. The numerical value of the stress exponent corresponds to what is observed for olivine [e.g., $(n+1)/(p+1) \sim 1.3$, *De Bresser et al.*, 2001]. The prefactor $\chi(T)$ does not vary too much in the mantle due to the competition between growth and recrystallization (e.g., corresponding to a small effective activation energy of order $(E_g - E_1)/(p+1)$) balanced by the partitioning factor f, see equation (10). The term $\chi(T)$ varies by a factor 4 at typical mantle conditions (1200-2100 K) and is minimal at 1600 K.

The relation (9) is valid in both dislocation regime and diffusion regime. As discussed in *Rozel et al.* [2010], this results from two causes. First, some of the strain rate is still accommodated by dislocation even for grains in the diffusive regime (see equation (11)), second, the largest grains of the grain size distribution can still remain in the dislocation regime even though the average grain size is in the diffusion domain.

The piezometric equilibrium (equation (9)) leads to a simple and important result developed in *Rozel et al.* [2010]. At a given temperature, when the applied stress is high, the equilibrium grain size is small and is then likely to reach the diffusion regime. On the contrary, when the stresses are low, the equilibrium grain size is large and the rheology is located in the dislocation regime. This means that the viscosity is likely to reach its diffusion component at high stress (i.e., probably in the lithosphere) and to remain in dislocation creep at low stress (in the mantle).

2.2.2. Definition of the viscosity

I consider that the mantle is deformed with a composite rheology

$$\underline{\dot{\boldsymbol{\epsilon}}} = \underline{\dot{\boldsymbol{\epsilon}}}_1 + \underline{\dot{\boldsymbol{\epsilon}}}_2, \tag{11}$$

where the strain-rate tensor is due to dislocation creep $\underline{\dot{\boldsymbol{\epsilon}}}_1$ and diffusion creep $\underline{\dot{\boldsymbol{\epsilon}}}_2$,

$$\underline{\dot{\boldsymbol{\epsilon}}}_1 = A_1\tau^{n-1}\underline{\boldsymbol{\tau}} \tag{12}$$

and

$$\underline{\dot{\boldsymbol{\epsilon}}}_2 = A_2\mathcal{R}^{-m}\underline{\boldsymbol{\tau}}, \tag{13}$$

where τ is the second invariant of the stress tensor, n and m are experimental dimensionless constants, R is the Boltzmann constant and T is the temperature. Both rheologies are temperature dependent, i.e., $A_i = A_{i0}\exp(-E_i/RT)$.

The deformation by dislocation creep corresponds to an equivalent viscosity

$$\eta_1 = \frac{1}{2A_1}\tau^{1-n} = \frac{1}{2}A_1^{-\frac{1}{n}}\dot{\epsilon}^{\frac{1-n}{n}}, \tag{14}$$

where $\dot{\epsilon}$ is the second invariant of the strain rate tensor. In the diffusion regime, combining the stress-radius relation (9) with the strain rate-stress relation (13) the equivalent viscosity obeys a similar equation:

$$\eta_2 = \frac{1}{2A_2'}\tau^{1-n'} = \frac{1}{2}A_2'^{-\frac{1}{n'}}\dot{\epsilon}^{\frac{1-n'}{n'}}. \tag{15}$$

where

$$\begin{aligned} A_2' &= A_2\chi^{-m} \\ n' &= \frac{m(n+1)+p+1}{p+1}. \end{aligned} \tag{16}$$

For simplicity, I used a stress exponent $n = 3$, which implies that $n' = 5$. Finally, the composite viscosity is defined by:

$$\frac{1}{\eta} = \frac{1}{\eta_1} + \frac{1}{\eta_2}. \tag{17}$$

The rheology at grain size equilibrium is therefore always non-linear. It is even more stress-dependent in the diffusion regime than in the dislocation regime ($n' > n$). This is in contradiction with the usual reasoning at constant grain size that confer stress non linearity to the dislocation regime and a Newtonian behavior to the diffusive regime.

In the following, I study the effect of this rheology on the convective dynamics of the mantle. The rheology and the grain size evolution parameters I use are only valid for olivine, i.e., for the major constituent of the shallowest mantle. I use this rheology for the whole mantle which is certainly a limitation of this model. However, the magnitude of the viscosity in the lower mantle is fixed by the Rayleigh number (see equation (5)) and is quantitatively acceptable.

2.3. Transition from diffusion to dislocation creep

The definition of the viscosity given by equation (17) is insufficient because the transition between diffusion and dislocation creep is not clear yet. The prefactor A_{20} of the viscosity in diffusion creep has to be defined. The following sections (2.3.1 and 2.3.2) explain how I chose to incorporate the diffusion creep rheology.

2.3.1. The dimensional stress transition

In the case of a mixture of diffusion and dislocation (see equation (17)), the rheological state of the fluid depends on

Table 1. Choice of parameters

Parameter	Value	Unit	Description
κ	10^{-6}	$m^2\ s^{-1}$	Thermal diffusivity
α	$3\ 10^{-5}$	K^{-1}	Thermal expansivity
ρ	5000	$kg\ m^{-3}$	Density
g	10	$m\ s^{-2}$	Gravity
h	2900	km	Domain depth
ΔT	1000	K	Temperature contrast
T_S	1000	K	Surface temperature
Ra_b	10^4		Bottom Rayleigh number
α_f	2		Coefficient of f
β	2.9		Coefficient of f
λ_2	2.054		Constant
λ_3	5.053		Constant
σ	0.6		GS distr. standard deviation
γ	1	$J.m^{-2}$	Surface tension
E_1	530	$kJ\ mol^{-1}$	Ref. Act. Energy (disl.)
n	3		disl. exponent
E_2	375	$kJ\ mol^{-1}$	Ref. Act. Energy (diff.)
m	3		diff. exponent
k_0	$4\ 10^4$	$\mu m^2\ s^{-1}$	Growth prefactor
E_g	200	$kJ\ mol^{-1}$	Growth activation energy
p	2		Growth coefficient
R	8.314	$J\ mol^{-1}\ K^{-1}$	Boltzmann constant

the magnitude of the stress. The transition stress τ_t between diffusion and dislocation creep is only a function of temperature. According to equations (14) and (15), I obtain :

$$\tau_t(T) = \left(\frac{A'_2(T)}{A_1(T)} \right)^{\frac{1}{n-n'}} . \quad (18)$$

When the stress in the fluid is greater than τ_t, then, at grain size equilibrium, creeps mainly occurs in the diffusion regime (i.e., recrystallization decreases the average grain size until deformation occurs by diffusion). When the stress is lower than τ_t, the viscosity is in the dislocation regime (i.e., grain growth proceeds until dislocation creep becomes dominant). This transition stress is only weakly temperature-dependent. High stress regions are usually located in the lithosphere where the viscosity is significantly increased by the low temperature. The deep mantle deforms in the dislocation regime and the shallow mantle deforms under diffusion.

However, as I previously mentioned, I cannot use the observed values of the activation energies and realistic top and bottom temperatures because of numerical convergence problems. The magnitude of the transition stress defined in equation (18) is affected by the rescaling of the activation energies. The choice of the activation energies and prefactors also imposes the reference bottom viscosity η_b (see equation (6)) and thus, the Rayleigh number of the simulation.

The transition stress would also be affected by a modification of the grain size growth law or of the partitioning factor f, as G and f enter in the expression of the piezometer (equation (10)) that ultimately controls the rheology through equation (16). Yet, the partitioning factor has been obtained according to the grain size evolution law (equation (7)) with experimental parameters. To remain consistent with experimental data, I chose not to modify its value. It could be argued that the grain size evolution law also depends on the dissipation term $\underline{\boldsymbol{\tau}} : \underline{\dot{\boldsymbol{\epsilon}}}_{dis}$ which is affected by the rescaling of the activation energies. Nevertheless, by imposing the bottom Rayleigh number which gives a realistic effective viscosity (significant of its expected value in the mantle), the orders of magnitude of the stress and strain-rate tensors are likely to remain in an acceptable range, at least in the convecting part. Thus, the modification of the activation energies of diffusion and dislocation creep has a weak impact on the effective grain size value reached in my simulations in the convective parts of the domain.

2.3.2. Rescaling of the rheological parameters

For consistency with experimental data, I have chosen to decrease the activation energies E_1 and E_2 by the same factor. As a reference, I used the experimental values E_1^{exp} and E_2^{exp} of *Hirth and Kohlstedt* [2003] (see Table 1). Thus, I use the constant ratio $E_2/E_1 = E_2^{exp}/E_1^{exp} \simeq 0.7$.

The dislocation creep viscosity is defined by the choice of the exponent n, the activation energy E_1 and the prefactor A_{10} or alternatively of n, E_1 and the bottom Rayleigh number (equation (6)), from which A_{10} can be readily deduced. For the diffusion creep, as I choose an activation energy $E_2 = 0.7E_1$, and keep the exponent m to 3, I only need a diffusion creep rheological prefactor A_{20} to complete my choice of parameters. As I cannot consider the experimental value of A_{20} because I have decrease the activation energies, it is safer to choose the stress at which the transition between diffusion and dislocation occurs, (equation (18)), which fixes the value of this prefactor.

In [*Rozel et al.*, 2010], we have shown that the grain size sensitive regime should be reached in the top lithosphere, using the experimental values of the rheological parameters, assuming a constant strain-rate of 10^{-15} s^{-1} and a temperature profile of a 50 Myrs old cooling lithosphere. In this simple setup, the top 50 kilometers of the lithosphere are in the diffusion regime. Thus, I can reasonably expect a rheological transition located in the lithosphere.

2.3.3. The dimensionless stress transition

The transition between diffusion and dislocation creep is controlled by the stress $\tau_t(T)$. Choosing a precise value for τ_t in Pa is impossible because it depends on temperature (equation (18)). Plus, the deviatoric stress level in a simulation is not known a priori. So, before using my diffusion creep model, for a given value of an activation energy, I run a first simulation assuming a simple dislocation creep rheology and record the maximal dimensionless deviatoric stress τ^*_{max}. This maximal stress is always reached at the top of the domain, at temperature T_s, it is then called $\tau^*_{max}(T_s)$.

Using this value, choosing the stress transition is easy because the maximal stress is reached at the surface, for a fixed temperature $T = T_s$. I define then the stress transition at the surface temperature T_s using (see figure 1)

$$\tau_t(T_s) = \Omega \tau_{max}(T_s), \quad (19)$$

where the dimensional maximal stress $\tau_{max}(T_s)$ is obtained from $\tau_{max}(T_s) = \tau^*_{max}(T_s)\dot{\epsilon}_0\eta_b$ (where ϵ_0 is again the reference strain rate used in equation 6) and Ω is a dimensionless number (hereafter called non dimensional stress). The dimensionless stress transition $\tau^*_t(T_s)$ is obtained with the same approach, such that $\tau_t(T_s) = \tau^*_t(T_s)\dot{\epsilon}_0\eta_b$ and $\tau^*_t(T_s) = \Omega\tau^*_{max}(T_s)$. An example of stress profiles using this formalism is schematically illustrated in figure 1. In this figure, a typical temperature profile is assumed (increasing with depth). The red curve shows the transition stress between diffusion and dislocation creep, defined in equation 18, non dimensionalized. This stress is non-homogeneous because it depends on temperature. The black curve shows the stress profile obtained in dislocation creep at all depths. Note that the value $\tau^*_{max}(T_s)$ is reached at the surface only and has no meaning elsewhere. $\tau^*_{max}(T_s)$ is only used to

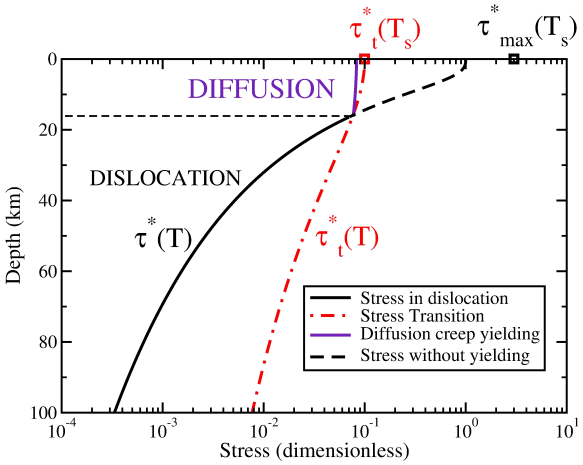

Figure 1. Schematic example of the stress profiles with and without the grain size dependent rheology. The black curve represents the stress profile in the reference simulation considering dislocation creep only. The red dot-dash curve shows the (temperature-dependent) transition stress profile I would obtain for $\Omega = \tau^*_t(T_s)/\tau^*_{max}(T_s) = 1/30$. The purple curve represents the stress profile reached with the composite rheology. The diffusion creep rheology acts as a stress limiter in the top lithosphere. Note that $\tau^*_{max}(T_s)$ is not reached by the black curve because it is the maximal value of the stresses in the domain, which is greater than the maximal value of the stress profile.

define the stress transition $\tau_t^*(T_s)$, which allows to define $\tau_t^*(T)$, for all T. The purple curve shows what the stress profile would be if the diffusion creep rheology were introduced in this example.

Using the equations 16, 18 and 19, it is possible to finally define the missing prefactor of the diffusion creep rheology:

$$A_{20} = (\Omega \tau^*_{max} \dot{\epsilon}_0 \eta_b)^{n-n'} \left(\frac{3\gamma G(T_S)\lambda_2}{pf(T_S)\lambda_3} \right). \quad (20)$$

When $\Omega < 1$, a temporarily or permanent grain size sensitive creep layer appears in the top boundary layer and may even reach the convecting mantle. When $\Omega > 1$, the diffusion creep rheology does not affect too much the convection. This formulation allows then to easily introduce the grain size dependence of the rheology in the lithosphere, as it is expected using experimental parameters [*Rozel et al.*, 2010].

With all these complexities in mind, I hope to provide a set of models that capture some of the complexities of the terrestrial planets: a mantle convecting with a composite rheology and where grain size is controlled by a piezometer with weak temperature dependence.

3. Results

3.1. Map of the convection regimes

I have performed a set of convection simulations for different values of the activation energy E_1 and different non dimensional stress Ω. The convection regimes reached in each simulation is presented in figure 2. The activation energy for dislocation creep, E_1, ranges from 250 kJ mol^{-1} to 420 kJ mol^{-1} and Ω from 10^{-3} to 10^3. When Ω is large, the rheology is everywhere controlled by dislocation creep (with an exponent of $n = 3$), when Ω is small the rheology is everywhere controlled by diffusion creep (which is grain size sensitive with an exponent $m = 3$, but appears as stress-dependent with an exponent $n' = 5$, because grain size and stress remain related by a piezometric rule).

The figure 2 shows that the introduction of a grain size dependent rheology is sufficient to break the stagnant lid generated in fully dislocation creep simulations. In itself, this result has a very important impact on the dynamics of planets. I show that a very high activation energy may be considered in diffusion creep without generating a stagnant lid. The diffusion creep rheology being very non-Newtonian, the temperature dependence of the viscosity is largely decreased by the large stress exponent $n = 5$ (see the exponents to the rheological prefactors in equations (14) and (15)).

Moreover, I also present the first episodic regime ever observed with fully viscous rheologies (and no ad hoc plastic yielding). The present model may actually represent plastic yielding very well and has the advantage of being based on an identified physical mechanism. This regime is suspected to be active on Venus, which has experienced an overturn within the past gigayear [*Nimmo and McKenzie*, 1998]. Also, this episodic regime (described in section 3.2.3) is located in a large region in the parameter space depicted in figure 2. It is then reasonably expectable in a realistic situation.

The figure 3 displays the Nusselt numbers obtained in all simulations, when the time dependent parameters have reached their (stationary or unstationary) equilibrium. I show that the convection regimes generated by the grain size-dependent rheology largely modifies the Nusselt number (heat flux). A clear trend to large Nusselt numbers is observed for increasing importance of the grain size (when Ω decreases). This means that the consideration of diffusion creep may largely increase the cooling rate of planets. This

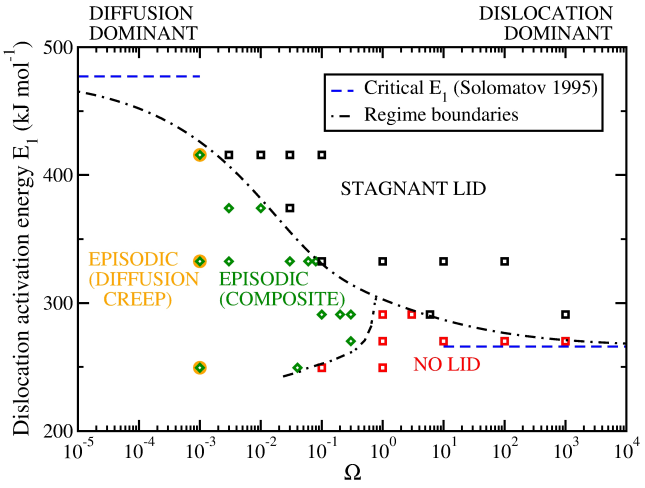

Figure 2. Convection regimes generated by my models. The boundaries between stagnant lid and isoviscous convection predicted by *Solomatov* [1995] are represented by the blue dashed lines. When the non dimensional transition stress Ω is decreased, the boundary between no lid or episodic and stagnant lid convection occurs at higher viscosity contrasts. At intermediate values of the transition stress, the system reaches an episodic regime. At low values of the transition stress, the whole mantle deforms in the diffusion regime but the convection regime remains episodic.

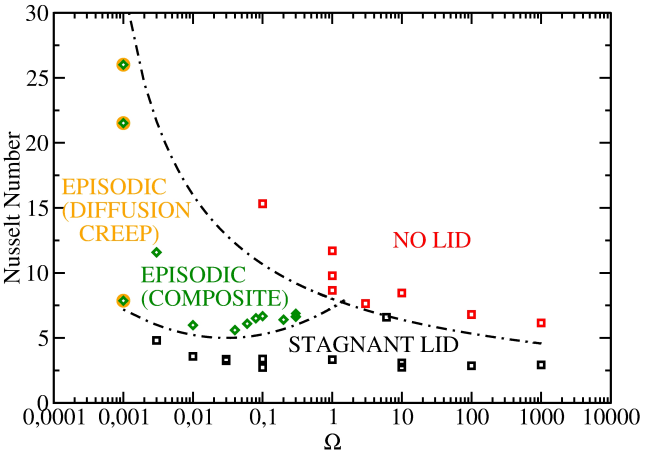

Figure 3. Regime diagram in the $\Omega - Nusselt$ space. The average Nusselt number is computed for a long time corresponding to a large number of overturns. Following the color code of Figure 2, black squares: stagnant lid regime, red squares: no lid regime, green diamonds: episodic regime and orange circles: episodic regime in diffusion creep. I show that the Nusselt numbers are affected by the modification of convection regimes.

result is not surprising, an increase of heat flux has been reported in the episodic regime obtained with plastic yielding [*Moresi and Solomatov*, 1998]. However, here, I did not consider any ad hoc plastic yielding. To summarize, a low heat flux is observed in the stagnant lid regime, an intermediate heat flux is reported in the episodic regime and a large heat flux is observed in the no lid regime. In the episodic regime, as seen in figure 4, the instantaneous Nusselt is highly vari-

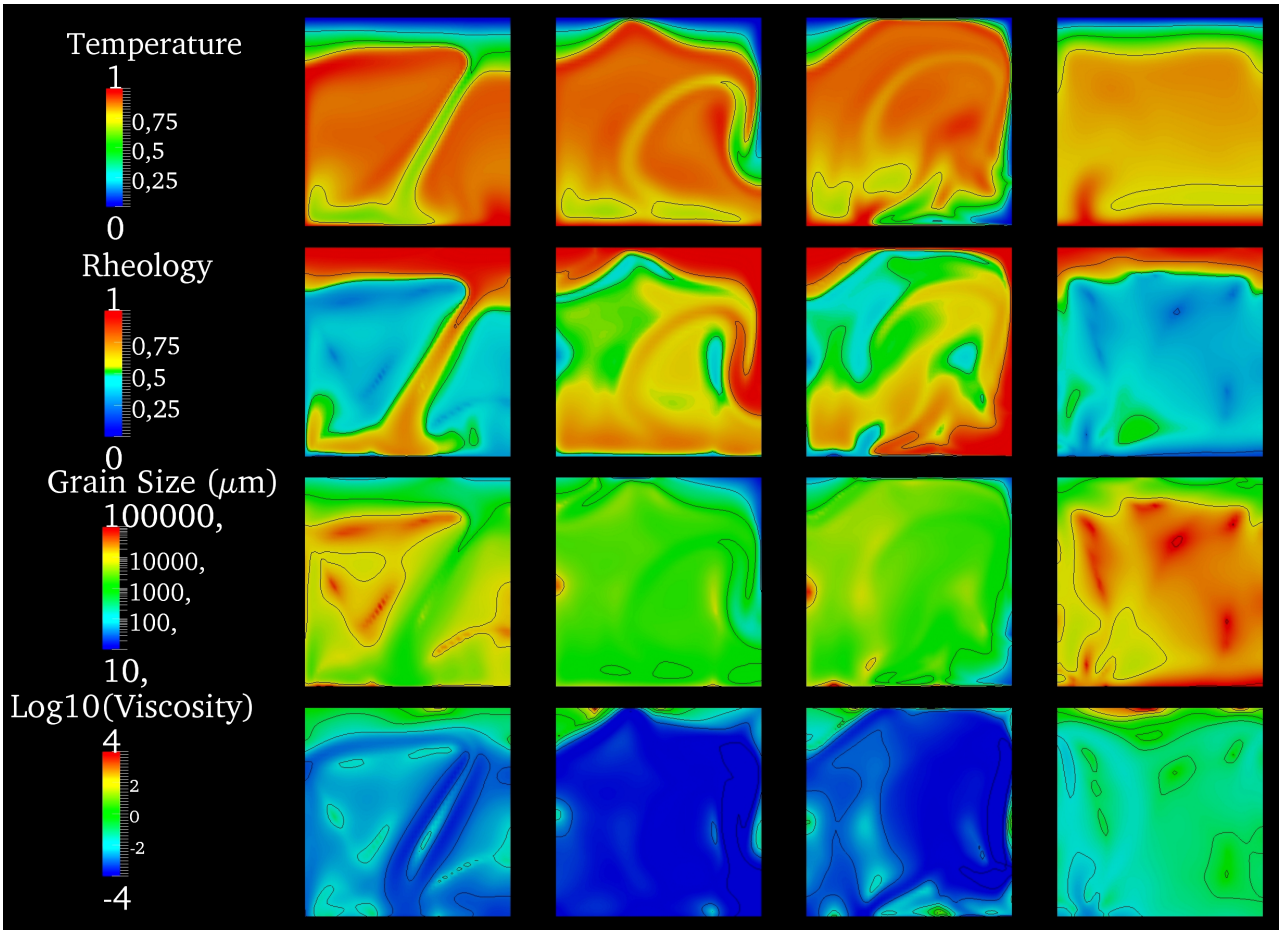

Figure 4. Episodic regime ($\Omega = 3\ 10^{-3}$, $E_1 = 374$ kJ mol^{-1}). The top thermal layer is always in the diffusion regime. The mantle oscillates between diffusion and dislocation creep following the activity of hot and cold plumes.

able and can be up to one order of magnitude larger or smaller than the average value. Finally, when the full diffusion regime is reached, the Nusselt number reaches very high values as the average viscosity becomes much smaller.

3.2. Description of the convection regimes

The figures 4 and 5 present the three main convection regimes obtained for various choices of parameters: stagnant lid, no lid and episodic regime. A description of these regimes is proposed in the present section.

3.2.1. Stagnant lid regime

In the stagnant lid regime, even if a grain size-dependent rheology is considered, the viscosity of the lithosphere remains sufficient to "freeze" the surface.

With large activation energies and in the two limiting cases $\Omega << 1$ and $\Omega >> 1$, the stagnant lid regime may be attained (illustrated in figure 5, left column). In this regime regime, I observe regions near the surface, in which the rheology is principally located in the diffusion creep regime (figure 5, left column). However, this diffusive layer is still too viscous to be broken by convection. In figure 5, I even show a case in which the whole lithosphere is in diffusion creep, without breaking the lid.

The stagnant lid regime has been largely documented in the past decades [*Morris and Canright*, 1984; *Fowler*, 1985; *Solomatov*, 1995; *Reese et al.*, 1998]. I did not focus this study on this precise regime but did not observe a significant modification of the dynamics of the flow field. The figure 5 shows that the grain size remains in a very acceptable range in this regime.

3.2.2. No lid regime

For a low activation energy and a large value of Ω, the temperature dependence of the viscosity is not sufficient to generate a stagnant lid (cf. figure 2, red squares at the bottom right). The figure 5 (right column) shows an example of this stationary regime.

Solomatov [1995] has shown that two distinct regimes may actually exist in absence of stagnant lid: the isoviscous and sluggish regimes. I only observed the sluggish regime in my computations. I show in section 3.3 that this is in agreement with the boundary layer theory formulated in *Solomatov* [1995].

The figure 5 (right column) shows that the internal dimensionless temperature is close to 0.7 and that the hot and cold plumes are not symmetrical. This is a clear confirmation that the no lid regime I observe is the sluggish (or also called "transitional") regime described by *Solomatov* [1995]. The grain size in the mantle is between 1 mm to 5 cm, which shows that the calibration is reasonable. The grain size in the top of the cold thermal layer reaches a very low value in this case (down to 1 micron). Though this value is small, it is still in an acceptable range. This small size is due to the large stresses that appear in the cold regions in which the viscosity is higher than in the mantle but where an important deformation is effective.

3.2.3. Episodic regime

I show in figure 4 the evolution with time (from left to right) of various quantities (temperature, rheology, grain size and viscosity) in the episodic regime. The corresponding Nusselt number evolution is depicted in figure 6 (where the blue stars indicate the moment at which I took the snapshots of figure 4). The rheology of the lithosphere oscillates between dislocation and diffusion creep stages depending on

its stress state. The behavior of the convective domain becomes cyclic. First, the lithosphere thickens with time while its rheology remains controlled by dislocation creep. The surface velocity and the Nusselt number decrease until the lithospheric deviatoric stresses become large enough to drive the rheology to the grain size sensitive creep regime. At this time, the lithosphere accelerates while the Nusselt number reaches a maximum (see figure 6) and the whole lithosphere sinks into the mantle. Then, the global convection weakens with a low level of deviatoric stresses that allow the grains to coarsen until the rheology becomes dominated by dislocations. The whole process is repeated without becoming strictly periodic. The figure 4 (third row) shows that the grain size in the mantle remains between 1 mm and 10 cm. In the lithosphere, the grain size is dynamically decreased from 1 mm down to 10 microns, which remains in an acceptable range. This shows that my calibration leads to a realistic situation, though I had to decrease the activation energies for technical reasons.

3.3. Regime boundaries

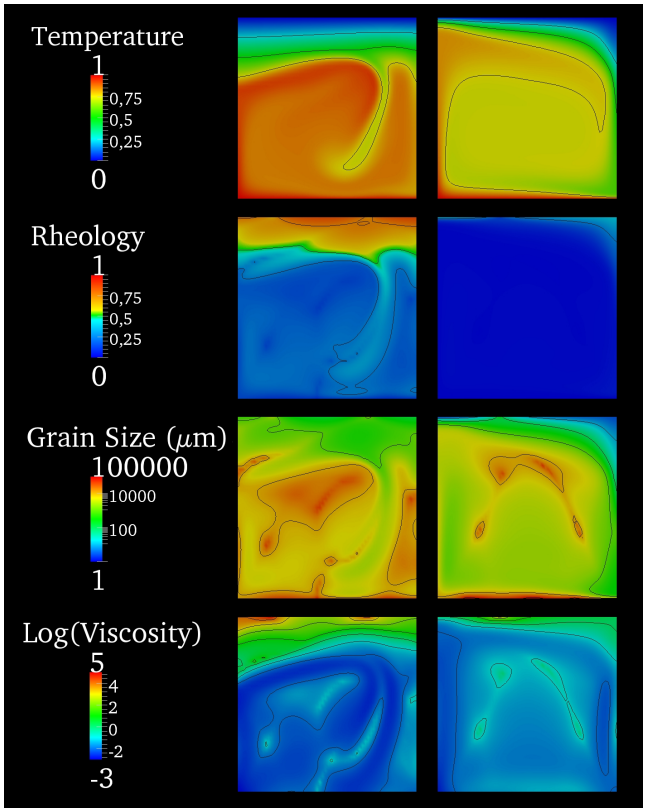

Figure 5. Stagnant lid (left, $\Omega = 3\ 10^{-2}$, $E_1 = 375$ kJ mol^{-1}) and no lid regime (right, $\Omega = 1$, $E_1 = 270$ kJ mol^{-1}). I plot temperature, rheology, grain size, and viscosity in each case. The rheology (second row) is represented in percentage of diffusion creep, from 0% (blue, for dislocation creep) to 100% (red, for diffusion creep). The diffusion creep is reached only in the lithosphere and for low Ω. On the left, the top layer is located in diffusion creep but the yielding is not sufficient to break the lid. On the right, the lithosphere is very fewly grain size-dependent but the lid as still been broken. The grain size (third row) remains in an acceptable range (from 1 micron to 10 cm). The viscosity varies over 8 orders of magnitude (in dimensionless units, in fourth row).

In this section, I explain how the end members of the boundaries of the convection regimes shown in figure 2 may be analytically derived using the boundary layer theory of *Solomatov* [1995]. In this theory, a stagnant lid is formed when:

$$\log\left(\frac{\eta\left(T_s,\tau_0\right)}{\eta\left(T_b,\tau_0\right)}\right) > 4(n+1), \tag{21}$$

where the viscosity ratio is actually the viscosity contrast through the convective domain for all stress τ_0. n is the stress exponent of the rheology. This equation defines the critical viscosity contrast above which the stagnant lid forms, for a given stress exponent n. These viscosities are obtained using the formulation of equation (14) and (15) at constant stress. The two following sections detail the end members of these boundaries in dislocation and diffusion dominant situations.

3.3.1. Dislocation creep dominant

In the case $\Omega >> 1$, the whole domain undergoes dislocation creep and the logarithm of the viscosity contrast is given by:

$$\log\left(\frac{\eta\left(T_s,\tau_0\right)}{\eta\left(T_b,\tau_0\right)}\right) = \log\left(\frac{A_1(T_b)}{A_1(T_s)}\right). \tag{22}$$

Using equation (21), the numerical values of Table 1 and $n = 3$, one can easily compute an activation energy which corresponds to the stagnant-sluggish boundary. The stagnant lid is formed for an activation energy E_1 greater than 266 kJ mol^{-1} (see the blue dashed line on the right in figure 2).

In the reference simulations (which completely exclude diffusion creep to obtain the maximal stress, as explained in section 2.3.1) I observe that the boundary between transitional and stagnant lid regimes is exactly located at $E_1 \simeq$ 266 kJ mol^{-1}.

Solomatov [1995] also provides an equation similar to equation (21) for the transition from isoviscous to sluggish regime. This boundary depends on the bottom Rayleigh number, which is not the case of the boundary with stagnant lid. Again, using the parameters of Table 1, the transition from transitional (sluggish) to isoviscous regime is located

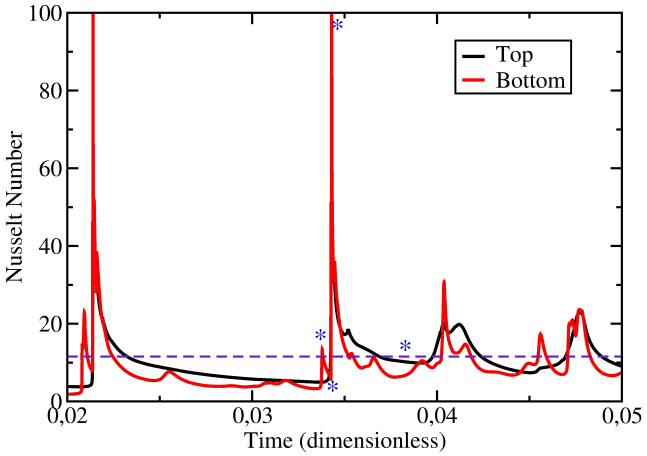

Figure 6. Top and bottom Nusselt numbers in the episodic regime as a function of time (from left to right) ($\Omega = 3\ 10^{-3}$, $E_1 = 374$ kJ mol^{-1}). I show that the Nusselt number reaches very high values when the cold boundary layer detaches and sinks in the mantle. The star symbols indicate the times at which the snapshots of figure 4 are taken. The dashed line show the average value I obtained in this case.

at $E_1 \simeq 184$ kJ mol^{-1}. The isoviscous regime is then never reached in the computations presented here.

3.3.2. Diffusion creep dominant

When $\Omega < 1$, as previously explained, the top of the domain is located in diffusion creep. In this case, the viscosity of the mantle can be obtained using the Rayleigh number and the parameters of Table 1. However, for $\Omega << 1$, the diffusion creep layer may reach the whole mantle. In this case, the viscosity of the whole mantle is decreased because the diffusion creep rheology becomes dominant. Then, the Rayleigh number defined in equation (5) does not allow to compute directly the viscosity of the mantle anymore.

For $\Omega << 1$, I can then assume that the whole domain undergoes diffusion creep only, which means that the viscosity contrast becomes

$$\log\left(\frac{\eta\left(T_s,\tau_0\right)}{\eta\left(T_b,\tau_0\right)}\right) = \log\left(\frac{A_2'(T_b)}{A_2'(T_s)}\right). \tag{23}$$

With $n' = 5$, the boundary between sluggish and stagnant lid regime corresponds to an activation energy for diffusion $E_2 = 337$ kJ mol^{-1}. As I perform my simulations with a constant ratio $E_2/E_1 = 0.7$, this situation should occur when I use $E_1 = 480$ kJ mol^{-1} (blue dashed line on the left in figure 2). Unfortunately, I did not observe this boundary because it is located beyond the borders of the parameter space reachable by the Stokes solver.

For very low values of the transition stress (non dimensional stress $\Omega = 10^{-3}$, Figure 2), due to convergence issues, I have only been able to observe the boundary between episodic and full diffusion creep. In these simulations, the whole mantle is located in the diffusion regime most of the time but resurfacing events still occur. When the activity of convection is low and stresses drop to a small value, the mantle can still reach dislocation creep for a very small time before the convection restarts.

The transition between sluggish and isoviscous creep in the diffusion regime is more difficult to compute because, as previously mentioned, the corresponding viscosity contrast depends on the bottom Rayleigh number [*Solomatov*, 1995]. In the diffusion creep regime, the bottom Rayleigh number may be computed using the definition of the composite viscosity but the viscosity may not be a perfectly monotonous function of temperature because of the temperature-dependent calibration of the piezometric relation. The analytical definition of the viscosity contrast in this case would then be more hazardous. Moreover, the full diffusion creep regime is not observed in my computations, which always remain in the episodic regime, even for a the smallest Ω. This means that an end-member computation neglecting dislocation creep would not be applicable.

Yet, a first order approximation of the diffusion creep rheology, in which I neglected the temperature-dependence of the rheological prefactor χ, defined in equation (10), shows that the isoviscous regime may potentially be reached for very small Ω and high activation energy (top left region in figure 2). However, regarding the high internal temperatures and the asymmetrical geometry of the plumes in the concerned simulations, I observe that the sluggish regime is always chosen by the composite and time-dependent rheology. So, though an isoviscous-stagnant lid transition may exists in the full diffusion creep regime, it is not reached in the parameter range I explored.

4. Discussion

The episodic regime had already been observed in simulations including plastic yielding but was always located in very narrow range of parameters. In [*Moresi and Solomatov*, 1998; *Stein et al.*, 2004] a variation of the yield stress by a factor 2 is sufficient to bring the convection regime back from episodic to stagnant or mobile lid. On the contrary, in the present study, this regime is rather easily reached. The transition stress between diffusion and dislocation creeps Ω can be modified on several orders of magnitude without bringing the convection back entirely in mobile or stagnant lid.

The new model investigated here is different from the usual plastic yielding formalism because no ad hoc stress limiter is imposed. However, the transition between dislocation and diffusion creep is very similar to a stress limiter because the viscosity is actually decreased when the diffusion regime is reached. So the present study shows that grain size reduction could be the mechanism responsible for plastic yielding in the lithosphere.

The present approach also provides a link between a microscopic behavior observed in the laboratory, the grain size, and the macroscopic behavior of the mantle. Several parameters might have a significant impact on the convection regimes. However, the wide range of parameter space in which I find the episodic regime shows that the grain size assisted episodic overturns are likely to happen in telluric planets. The incorporation of the non-equilibrium grain size dynamics (i.e., solving for $d\mathcal{R}/dt$ in equation (7) rather than assuming steady state), is unlikely to modify by itself the behavior of the mantle as the time of equilibration are short [*Rozel et al.*, 2010] (at least using the experiments of *Karato* [1989]). In a real polycrystalline mantle, the various phases should slow down the grain growth [*Bercovici and Ricard*, 2012]. This phenomenon is generally known as Zener pinning [*Smith*, 1948] and is documented for olivine-pyroxene mixtures [*Hiraga et al.*, 2010]. However the evolution of grain growth at very long time does not really affect my simulations: in the deep mantle, as soon as grains are large enough to deform under dislocation the rheology becomes independent of their sizes.

Another limitation of this model could be the fact that a sufficient amount of stress is necessary to activate dislocation creep [*Weertman and Weertman*, 1992]. If this critical stress is not reached, deformation can still be accommodated in diffusion creep. In the case of the episodic regime, when convection almost stops after an overturn, the stresses drop to a very small value. In this model, the grain size increases to large values because it is directly linked to the stresses. The rheology switches then instantaneously to dislocation creep. If we consider that a sufficient stress must be reached before the activation of dislocation creep, it means that the convection will restart in diffusion creep. But anyhow, the stress will increase with the restart of convection and it is likely that the sufficient amount of stress needed to activate dislocation creep will be reached. Considering this threshold effect would probably slightly change the dynamics of the episodic regime, but would not affect much the whole convection regime. However, this phenomenon is not the only one which can add some complexity to the new model I propose. The idea that the density of dislocations is directly linked to the stress state is a big simplification of the dislocation dynamics. From this point of view, the model proposed in *Rozel et al.* [2010] is very simple but I show here that it is sufficient to affect the convection styles of planets in itself, even without considering the full complexity of dislocation dynamics.

The grain size-dependent rheology presented in this paper seems to be insufficient to produce a plate-like behavior by itself. It is at least missing a memory and solving for the time dependence of the grain size seems to provide a too fast healing. A multiphase rheology that includes Zener pinning might allow the necessary slower rheology. A free surface and the consideration of other rheologies (grain boundary sliding or Peierls creep) could also have a non-negligible impact on the convection regimes.

5. Conclusion

I have tested the new grain size equilibrium state predicted in a previous paper [*Rozel et al.*, 2010] in a set of numerical simulations of mantle convection. I compute a composite viscosity calibrated for olivine using experimental data allowing both dislocation and diffusion creep regimes, depending on the stress state. Although, for numerical reasons, I cannot use the exact observed parameters, I tried to remain as close as presently possible from the experimental observations. The grain size and viscosities used in the simulations presented here are always in an acceptable range.

I showed that a grain size-dependent rheology dramatically affects the convection regime of the telluric planets. The rheology derived by *Rozel et al.* [2010] is sufficient to break the stagnant lid for a wide range of parameters. In most cases, the convection regime reaches an episodic behavior composed of resurfacing events that might be relevant to the evolution of Venus. I show that the cooling rate of the mantle is largely influenced by the consideration of an experimentally calibrated grain size-dependent rheology.

Acknowledgments. Support was provided by the CNRS (grant INSU-PNP), the US Nation Science Foundation Grant EAR 1015229, the Marie Curie Initial Training Network TOPOMOD. I deeply thank Yanick Ricard for his support and his comments on the present manuscript. I also thank the anonymous reviewer and Louis Moresi for their very interesting and constructive feedback on the present manuscript.

References

Austin, N. J., and B. Evans (2007), Paleowattmeters: A scaling relation for dynamically recrystallized grain size, *Geology*, *35*, 343–346.

Barr, A., and W. B. McKinnon (2007), Convection in ice i shells and mantles with self-consistent grain size, *Journal of Geophysical Research-Planets*, *112*, doi:10.1029/2006je002781.

Bercovici, D. (1993), A simple model of plate generation from mantle flow, *Geophys. Journ. Int.*, *114*(3), 635–650.

Bercovici, D., and S. Karato (2003), Theoretical analysis of shear localization in the lithosphere, in *Reviews in Mineralogy and Geochemistry: Plastic Deformation of Minerals and Rocks*, vol. 51, edited by S. Karato and H. Wenk, chap. 13, pp. 387–420, Min. Soc. Am., Washington, DC.

Bercovici, D., and Y. Ricard (2003), Energetics of a two-phase model of lithospheric damage, shear localization and plate-boundary formation, *Geophys. J. Intl.*, *152*, 581–596.

Bercovici, D., and Y. Ricard (2012), Mechanisms for the generation of plate tectonics by two-phase grain-damage and pinning, *Phys. Earth Planet. Int.*, *in press*.

Bercovici, D., Y. Ricard, and M. Richards (2000), The relation between mantle dynamics and plate tectonics: A primer, in *History and Dynamics of Global Plate Motions, Geophys. Monogr. Ser.*, vol. 121, edited by M. A. Richards, R. Gordon, and R. van der Hilst, pp. 5–46, Am. Geophys. Union, Washington, DC.

Braun, J., J. Chery, A. Poliakov, D. Mainprice, A. Vauchez, A. Tomassi, and M. Daignieres (1999), A simple parameterization of strain localization in the ductile regime due to grain size reduction: A case study for olivine, *J. Geophysical Research-solid Earth*, *104*, 25,167–25,181.

Burg, J.-P., and S. Schmalholz (2008), Viscous heating allows thrusting to overcome crustal-scale buckling: Numerical investigation with application to the himalayan syntaxes, *Earth and Planetary Science Letters*, *274*(1-2), 189 – 203, doi:DOI: 10.1016/j.epsl.2008.07.022.

Christensen, U. (1989), Mantle rheology, constitution, and convection. mantle convection, in *Plate Tectonics and Global Dynamics*, edited by P. W. R, pp. 595–655, New York: Gordon and Breach Sci. Publish.

De Bresser, J., J. T. Heege, and C. Spiers (2001), Grain size reduction by dynamic recrystallization: can it result in major rheological weakening?, *Int. J. Earth Sciences*, *90*, 28–45.

Duretz, T., T. V. Gerya, and D. A. May (2010), Numerical modelling of spontaneous slab breakoff and subsequent topographic response, *Tectonophysics*, *In Press, Corrected Proof*, –, doi: DOI: 10.1016/j.tecto.2010.05.024.

Foley, B. J., D. Bercovici, and W. Landuyt (2012), The conditions for plate tectonics on super-earths: Inferences from convection models with damage, *Earth and Planetary Science Letters*, *331332*(0), 281 – 290, doi:10.1016/j.epsl.2012.03.028.

Fowler, A. C. (1985), Fast thermoviscous convection, *Stud. appl. math.*, *72*, 189–219.

Hall, C., and E. Parmentier (2003), Influence of grain size evolution on convective instability, *Geochem. Geophys. Geosyst.*, *1029*(4), doi:10.1029/2002GC000308.

Harlow, F., and J. Welch (1965), Numerical calculation of time-dependent viscous incompressible flow of fluid with a free surface, *Phys. Fluids*, *8*(2182).

Hilairet, N., B. Reynard, Y. Wang, I. Daniel, S. Merkel, N. Nishiyama, and S. Petitgirard (2007), High-pressure creep of serpentine, interseismic deformation, and initiation of subduction, *Science*, *318*(5858), 1910–1913, doi: 10.1126/science.1148494.

Hillert, M. (1965), On theory of normal and abnormal grain growth, *Acta Metallurgica*, *13*, 227–230.

Hiraga, T., C. Tachibana, N. Ohashi, and S. Sano (2010), Grain growth systematics for forsterite enstatite aggregates: Effect of lithology on grain size in the upper mantle, *Earth and Planetary Science Letters*, *291*(14), 10 – 20, doi: 10.1016/j.epsl.2009.12.026.

Hirth, G., and D. Kohlstedt (2003), Rheology of the upper mantle and the mantle wedge: a view from the experimentalists, in *Subduction Factor Mongraph*, vol. 138, edited by J. Eiler, pp. 83–105, Am. Geophys. Union, Washington, DC.

Kameyama, M., D. A. Yuen, and H. Fujimoto (1997), The interaction of viscous heating with grain-size dependent rheology in the formation of localized slip zones, *Geophys. Res. Let.*, *24*, 2523–2526.

Kameyama, M., D. A. Yuen, and S.-I. Karato (1999), Thermal-mechanical effects of low-temperature plasticity (the peierls mechanism) on the deformation of a viscoelastic shear zone, *Earth and Planetary Science Letters*, *168*(1-2), 159 – 172, doi: DOI: 10.1016/S0012-821X(99)00040-0.

Karato, S.-I. (1989), Grain growth kinetics in olivine aggregates, *Tectonophysics*, *168*, 255–273.

Lenardic, A., and W. M. Kaula (1994), Selflubricated mantle convection: Twodimensional models, *Geophys. Res. Lett.*, *21*(16), 1707–1710.

McKenzie, D. (1984), The generation and compaction of partially molten rock, *J. Petrol.*, *25*, 713–765.

Montési, L., and M. Zuber (2002), A unified description of localization for application to large-scale tectonics, *J. Geophys. Res.*, *107*(B3), doi:10.1029/2001JB000465.

Montési, L. G. J., and G. Hirth (2003), Grain size evolution and the rheology of ductile shear zones: from laboratory experiments to postseismic creep, *Earth and Planetary Science Letters*, *211*, 97–110.

Moresi, L., and V. Solomatov (1998), Mantle convection with a brittle lithosphere: Thoughts on the global tectonic style of the earth and venus, *Geophys. J.*, *133*, 669–682.

Morris, S., and D. Canright (1984), A boundary-layer analysis of benard convection in a fluid of strongly temperature-dependent viscosity, *Phys. Earth Plan. Int.*, *36*, 355–373.

Nimmo, F., and D. McKenzie (1998), Volcanism and tectonics on venus, *Annu. Rev. Earth Planet. Sci.*, *26*, 23–51.

Ogawa, M., G. Schubert, and A. Zebib (1991), Numerical simulations of three-dimensional thermal convection in a fluid with strongly temperature-dependent viscosity, *Journal of Fluid Mechanics Digital Archive*, *233*(-1), 299–328, doi: 10.1017/S0022112091000496.

Patankar, S. (1980), *Numerical Heat Transfer and Fluid Flow*, McGraw-Hill, New York.

Post, A., and J. Tullis (1999), A recrystallized grain size piezometer for experimentally deformed feldspar aggregates, *Tectonophys.*, *303*, 159–173.

Reese, C. C., V. S. Solomatov, and L.-N. Moresi (1998), Heat transport efficiency for stagnant lid convection with dislocation viscosity: Application to mars and venus, *Journ. Geophys. Res.*, *103*, 13,643–13,657.

Ricard, Y., and D. Bercovici (2009), A continuum theory of grain size evolution and damage, *J. Geophys. Res.*, *114*, B01,204.1–B01,204.30.

Rozel, A., Y. Ricard, and D. Bercovici (2010), A thermodynamically self-consistent damage equation for grain size evolution during dynamic recrystallization, *Geophysical Journal International*, doi:10.1111/j.1365-246X.2010.04875.x.

Shimizu, I. (2008), Theories and applicability of grain size piezometers: The role of dynamic recrystallization mechanisms, *Jour. Struct. Geol.*, *30*, 899–917.

Smith, C. (1948), Grains, phases, interfaces: an interpretation of microstructures, *Trans. Met. Soc. AIME*, *175*, 15–51.

Solomatov, V., and C. Reese (2008), Grain size variations in the earth's mantle and the evolution of primordial chemical heterogeneities, *J. Geophys. Res.*, *113*, doi:10.1029/2007JB005319.

Solomatov, V. S. (1995), Scaling of temperature- and stress-dependent viscosity convection, *Phys. Fluids*, *7*, 266–274.

Stein, C., J. Schmalzl, and U. Hansen (2004), The effect of rheological parameters on plate behaviour in a self-consistent model of mantle convection, *Phys. Earth. and Plan. Int.*, *142*, 225–255.

Tackley, P. J. (2000), Self consistent generation of tectonic plates in time-dependent, three dimensional mantle convection simulations, part 1: Pseudoplastic yielding, *G3*, *1*.

Trompert, R., and U. Hansen (1996), The application of a finite volume multigrid method to three-dimensional flow problems in a highly viscous fluid with a variable viscosity, *Geophys. Astrophys. Fluid Dyn.*, *83*, 261–291.

Trompert, R., and U. Hansen (1998), On the rayleigh number dependence of convection with a strongly temperature-dependent viscosity, *Phys. Fluids*, *10*, 351–360.

Van der Wal, D., P. Chopra, M. R. Drury, and J. D. Fitzgerald (1993), Relationships between dynamically recrystallized grain size and deformation conditions in experimentally deformed olivine rocks, *Geophys. Res. Lett.*, *20*, 1479–1482.

Weertman, J., and J. Weertman (1992), *Elementary Dislocation Theory*, 232 pp., Oxford University Press, USA.

Weinstein, S. A., and P. L. Olson (1992), Thermal convection with non-newtonian plates, *Geophys. J. Intl.*, *111*, 515–530.

A. Rozel, [1]LET Laboratory of Experimental Tectonics, Dipartimento Scienze Geologiche, Università Roma TRE,
L.S.L. Murialdo 1; 00146 Roma, Italy. (antoinerozel@gmail.com)